New Test of QED from a Measurement of the $4^2S_{1/2}$-$4^2F_{5/2}$ Three-Photon Transition in He^+

P. K. Majumder[a] and F. M. Pipkin

Lyman Laboratory, Harvard University, Cambridge, Massachusetts 02138

(Received 3 April 1989)

A new three-photon separated-oscillatory-field microwave-resonance technique has been employed to measure the $4^2S_{1/2}$-$4^2F_{5/2}$ fine-structure interval in He^+ with an accuracy of 4 ppm. The indirect result for the He^+ ($n=4$) Lamb shift is $\mathcal{L}=1768.732(124)$ MHz. This 70-ppm measurement provides the most precise Lamb-shift determination in any hydrogenic ion or atom outside of the $n=2$ manifold. This experimental result is in excellent agreement with the theoretical value based on Mohr's calculation of the ($n=2$) binding correction.

PACS numbers: 35.10.Fk

Measurements of the Lamb shift in hydrogenic systems provide sensitive tests of quantum electrodynamics (QED). In hydrogen, however, significant discrepancies in the measured radius of the proton limit the sensitivity for testing QED.[1] Conversely, in $^4He^+$, the uncertainty in the theoretical predictions is dominated by higher-order binding correction terms $[G_{SE}(Z\alpha)]$ in the QED expansion. Two recent measurements of the $2^2S_{1/2}$-$2^2P_{1/2}$ Lamb shift[2,3] in He^+ show excellent agreement with Mohr's calculation of the binding correction.[4] However, all high-precision measurements of Lamb-shift intervals have thus far been limited to the $n=2$ manifold. While it is expected that the Lamb shift scales as Z^4/n^3, there is the possibility of additional n dependence in the term $G_{SE}(Z\alpha)$.

This paper reports a 70-ppm measurement of the Lamb shift in the $n=4$ manifold of He^+ by a new technique which uses multiphoton excitation in conjunction with the method of separated oscillatory fields. This three-photon measurement of the 27-GHz $4^2S_{1/2}$-$4^2F_{5/2}$ interval has several advantageous features. First, due to the relatively long F-state lifetime, the natural linewidth in a fast-beam experiment is 24 MHz. This is nearly an order of magnitude less than the 200-MHz linewidth for the 1.768-GHz $4^2S_{1/2}$-$4^2P_{1/2}$ Lamb-shift transition. Second, the narrow tuning range required to observe this transition makes the line-center determination relatively insensitive to asymmetries and nonidealities in the microwave electric field used to drive the transition. Such asymmetries have often been the limiting systematic uncertainty in the determination of the line center for the broad resonances associated with S-P transitions. Third, at this high frequency there are no overlapping resonances in higher n states.

Figure 1 shows the energy-level diagram for the $n=4$ manifold of He^+. The arrows indicate the three-photon transition from the initial $4^2S_{1/2}$ state to the final $4^2F_{5/2}$ state. Because of the large energy defects associated with the virtual intermediate P and D states, a large microwave electric field is required to drive this transition. As a result there is a large, nonlinear ac Stark shift for all of the He^+ ($n=4$) levels. For precise extrapolation of the measured interval to zero microwave field, it is necessary to understand completely the dependence of the ac Stark shifts on the microwave power.

He^+ ions were extracted from an rf discharge ion source and accelerated to 127 keV ($v=0.0083c$). Collisions with nitrogen in a differentially pumped cell excited the ions into higher excited states. The ions first passed through a "prequenching" region consisting of a fixed microwave cavity tuned to the $4^2S_{1/2}$-$4^2P_{3/2}$ transition at 20.180 GHz and then passed through the region of separated oscillatory fields (SOF). Figure 2 shows the X-band waveguide microwave apparatus. The microwaves exited the magic tee either in phase or π out of phase and were then incident on two interaction regions consisting of nearly identical tunable microwave cavities. Both forward and reflected power were monitored for each cavity. Dielectrically tunable, high-Q cavities were used to produce the ~300-V/cm microwave electric fields required to drive the three-photon transition with a modest input power (< 1 W/cavity). The He^+ ions entered the cavities through 3-mm-inner-diam cylindrical tubes centered in the broad face of the waveguide wall at an antinode of the electric field. Data were taken with

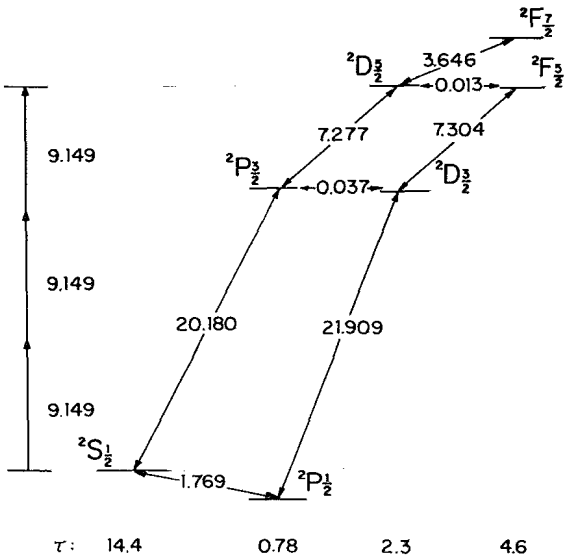

FIG. 1. Energy-level diagram for the $n=4$ manifold of He^+ showing the three-photon $4^2S_{1/2} \rightarrow 4^2F_{5/2}$ transition measured in this experiment. Intervals are in GHz; lifetimes, τ, in ns.

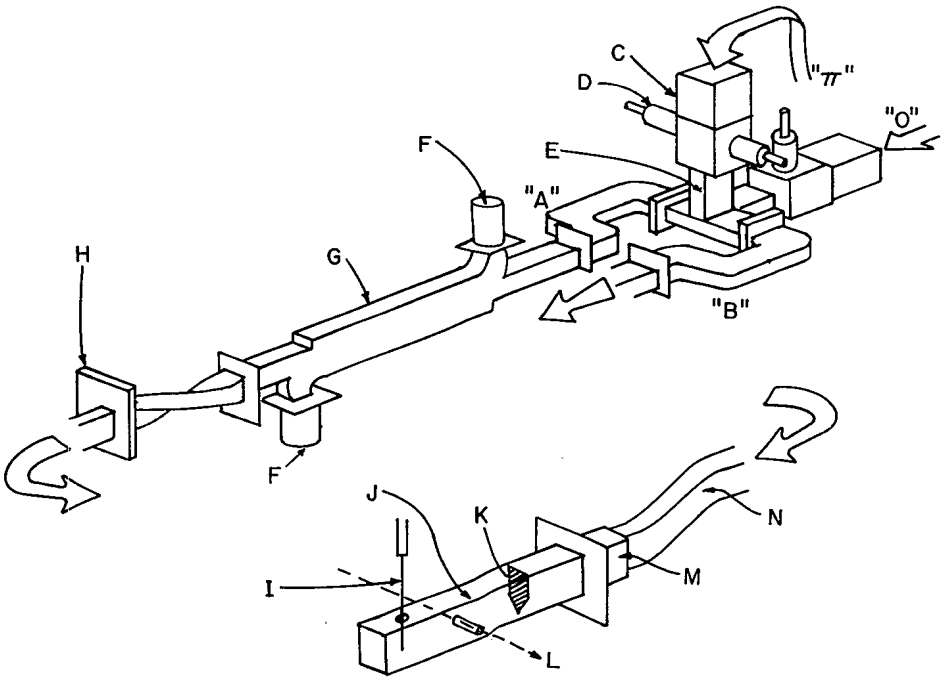

FIG. 2. Drawing of the X-band waveguide portion of the SOF microwave system from the magic tee inputs to the cavities. Only the "A" arm and interaction region of the two identical arms and interaction regions is shown. "0" and "π" denote the microwave inputs for the microwave fields in the two arms in and 180° out of phase, respectively. Labeled components: C, isolator; D, compound screw tuner; E, magic tee; F, thermistor; G, dual directional coupler, H, vacuum window; I, dielectric tuning rod; J, microwave cavity; K, iris; L, ion beam; M, entrance to vacuum chamber; N, guide offset.

nominal SOF separations of 30, 45, and 60 mm; the interaction length determined by the X-band waveguide was 10 mm. The $4^2S_{1/2}$ state population at the end of the SOF region was monitored with a large-solid-angle uv detector[5] which was sensitive to photons emitted in the decay $4^2S_{1/2} \rightarrow 2^2P_{1/2,3/2}$. Beam currents of roughly 10 μA were detected further downstream in a Faraday cup.

Detector, beam, and power level voltages were digitized by voltage-to-frequency converters, counted, and read into an IBM PC. The quench signals were calculated from the fractional decrease in light detected with the SOF microwaves on for each relative phase. The SOF "interference" signal is defined as the difference in these signals for in-phase and out-of-phase 9-GHz microwaves. The background component of the detected light was removed by use of the residual signals when the 20-GHz $4^2S_{1/2}$ state prequench was on.

Ramsey's method of separated oscillatory fields[6,7] was used to great advantage in this experiment. For this three-photon transition, the interference signal has the approximate analytic form

$$I(\omega,\omega_0,T,\tau,V) = A(\omega,\omega_0,\tau,V)e^{-(1/2)(\gamma_f-\gamma_s)(T+2\tau)} \times\cos[(3\omega-\omega_0)(T+\tau)] .$$

Here, τ is the atom-field interaction time, V is the transition matrix element, T is the time spent in the intermediate field-free region, ω is the applied microwave frequency, ω_0 is the three-photon resonant frequency $\Delta E(4^2S_{1/2}$-$4^2F_{5/2})/\hbar$, and γ_j is the inverse lifetime of state j. The first term represents the single-region quench envelope. For this experiment the width of the envelope is transit-time limited to roughly 60 MHz. The cosine modulation term, characteristic of the interference signal, has a width which is determined by the separation of the regions. For this experiment we were able to achieve slightly "subnatural" linewidths. The ability to vary the cavity separation, T, provides a valuable tool for investigating systematic uncertainties in a precision measurement. Furthermore, since the ion spends only a fraction of the measurement time in the microwave field, the ac Stark shift of the interference signal is smaller than for the analogous single-cavity experiment. Finally, at these wide separations, there are no one- or two-photon contributions to the interference signal.

Figure 3 shows typical data for the central lobe of the interference pattern with 30-mm separation at three microwave power levels. Eighty runs of this type were made at nine microwave power levels and three SOF separations. Data were taken in each configuration with the cavities and the microwave drive interchanged so as to cancel the effect of residual phase shifts due to physical or electrical path length differences in the two spectroscopy regions. Statistical fits of the data by a simple cosine function yielded line-center determinations with typical uncertainties of 25 kHz. Prior to further analysis the second-order Doppler-shift correction of 0.312(6) MHz was made for each measured line center.

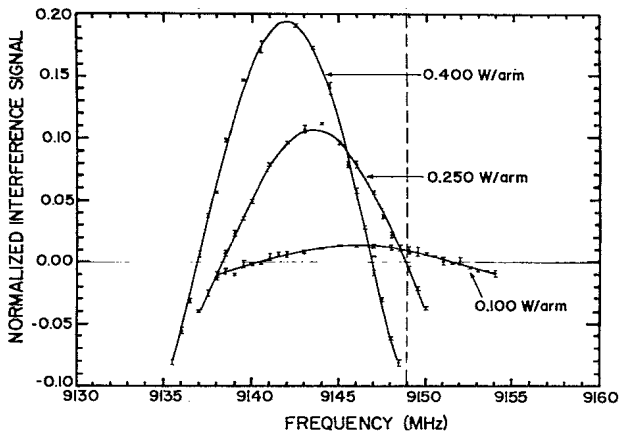

FIG. 3. Experimental interference signals with a nominal field separation of 30 mm at nominal microwave powers of 0.100, 0.250, and 0.400 W/arm. The vertical dashed line gives the extrapolation to zero microwave power.

In order to simulate the experimental measurement and gain information for extrapolation of the nonlinear power shift, we employed an extensive numerical procedure which integrates the Schrödinger equation for all 32 levels in the $n=4$ manifold for the case of microwave fields of arbitrary strength, spatial dependence, polarization, and relative phase. To determine the electric field shapes in the cavities, we first used the electrostatic approximation and numerically solved Laplace's equation in cylindrical coordinates to determine the longitudinal and transverse electric field in the entrance tubes and the waveguide. We confirmed the accuracy of these solutions by comparing them to an exact solution of Maxwell's equations for our geometry generated using a supercomputer.

The numerical accuracy of the integration procedure was checked by comparing the results with those of a totally different, equally precise method. The "Floquet" method, due to Shirley,[8] was used to transform the Hamiltonian (with periodic time dependence) into a time-independent matrix of infinite dimension. This provides a nonperturbative solution of the Schrödinger equation without resorting to the rotating-wave approximation. The absolute signal sizes predicted by the two methods agree to 0.01%; the power-shift predictions for a given field strength agree to better than 0.1%.

An extensive series of microwave measurements was used to relate the microwave electric field seen by the ions to the input microwave power. The net result was a determination of the absolute electric field for each cavity with an uncertainty of $\pm 1\%$.[9] Figure 4(a) shows a comparison of average quench and interference signals as a function of nominal input power for experiment and simulation. The accuracy with which the simulation (solid line) reproduces the data reinforces our confidence in the electric field calculation and the accuracy of the simulation.

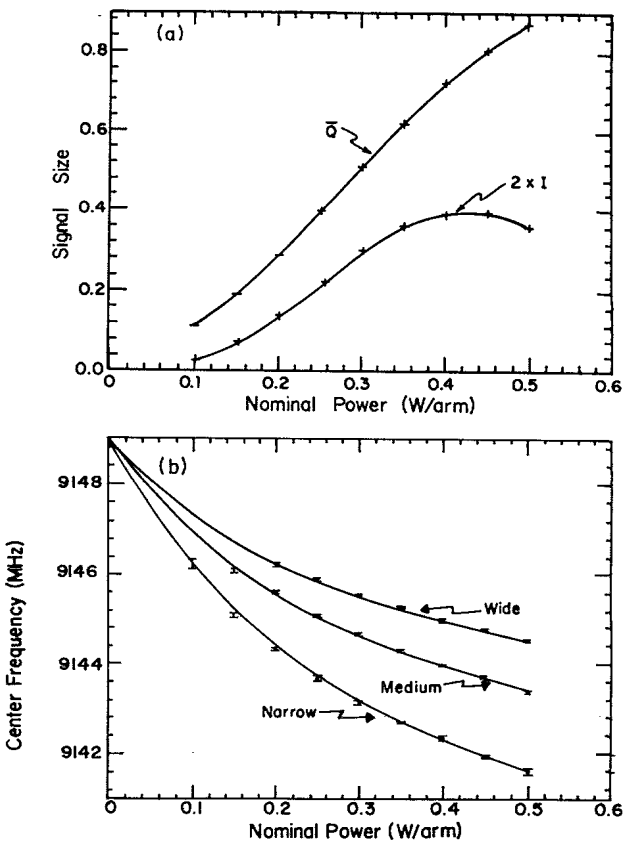

FIG. 4. (a) Comparison of the dependence of the quench and interference signals on microwave power for a field separation of 30 mm. The points are the experimental data; the solid lines the results of the simulation. (b) Comparison of measured and simulated power shifts for the three separations.

Figure 4(b) compares the experimental and simulated power shifts. The data used for the extrapolation consisted of 28 points comprising four distinct sets of three SOF separations (30, 45, and 60 mm, and 30 mm again). The zero-field intercept used in the simulations was the best theoretical estimate based on Mohr's calculation for $n=2$.

The final extrapolation used the simulated power-shift curves. We first fitted the simulated data by a cubic polynomial, the lowest order which gave acceptable fits. Independently we determined from the Floquet results that an analytic expansion of the power shift to order P^3 was sufficient for the field strengths used in this measurement. We next discarded the intercept assumed for the simulations and performed a one-parameter fit to the experimental data, allowing the simulation "template" to slide over the data until the best-fit intercept was determined.

Each of the four data sets was individually extrapolated to determine the zero-power intercept. The χ^2 for all the fits was 23.8 for 24 degrees of freedom. The statistical uncertainty of the mean intercept was taken to be the

TABLE I. A summary of the sources of uncertainty and final value for the $4^2S_{1/2}$-$4^2F_{5/2}$ fine-structure interval.

Source of uncertainty	Uncertainty (kHz)
Statistical (based on extrapolation)	29
Second-order Doppler shift	6
Microwave electric field strength	24
Envelope of microwave field	10
Residual microwave asymmetries	10
Stray dc electric fields	3
Stray magnetic fields	5
Residual first-order Doppler shift	1
Detector nonlinearity	3
Total uncertainty	41
Final average line center	9148.830(41) MHz
$\Delta E(4^2S_{1/2}$-$4^2F_{5/2})$	27446.490(124) MHz

standard deviation of the mean of the four independent results. Table I lists the mean and the important contributions to the overall uncertainty.

By combining our result for the $4^2S_{1/2}$-$4^2F_{5/2}$ fine-structure interval (Table I) with the theoretical value for the $4^2P_{1/2}$-$4^2F_{5/2}$ interval [29215.224(6) MHz], we obtain a 70-ppm determination of the He^+ ($n=4$) Lamb shift,

$$\mathcal{L}(\mathrm{He}^+(n=4)) = 1768.732(124)\ \mathrm{MHz}.$$

The agreement with the theoretical value, 1768.721(60) MHz, is excellent. It is possible to deduce an experimental value for the higher-order binding correction $G_{SE}(Z\alpha)$ for the $\mathcal{L}(\mathrm{He}^+(n=4))$ by subtracting away the remaining very well-known terms. From our measured value, we obtain $G_{SE}(Z\alpha) = -22.8(2.0)$. This agrees with the value Mohr obtained for $\mathcal{L}(\mathrm{He}^+(n=2))$ [$G_{SE}(Z\alpha) = -23.0(1.0)$] and suggests there is no strong dependence on n. A new calculation of $\mathcal{L}(\mathrm{He}^+(n=4))$ is needed to compare the measured n dependence with theory.

In summary, we have not only demonstrated the feasibility of using multiphoton transitions for precision measurements of fine-structure intervals but we have used this technique to measure with a precision comparable to that obtained in the $n=2$ manifold, the Lamb shift in the $n=4$ manifold of He^+.

We would like to thank H. A. Klein for aid and stimulating discussions in the early phase of this measurement, C. A. Perez for aid in taking data and calculating the simulated signals, L. Moorman for calculation of the electric field in the cavities with the MAFIA program at Brookhaven National Laboratory, and E. W. Hagley for aid in simulations carried out using the supercomputer. M. C. Brower and M. E. Poitzsch were helpful through innumerable discussions of the experiment. Gordon Drake provided aid in determining the best values for the fine-structure intervals in the $n=4$ manifold of He^+. We thank the John von Neumann National Supercomputer Center for allotment of time. This work was supported in part by National Science Foundation Grant No. PHY-8704527.

[a]Present address: Physics Department, University of Washington, Seattle, WA 98195.

[1]S. R. Lundeen and F. M. Pipkin, Metrologia **22**, 9 (1986).

[2]G. W. F. Drake, J. Patel, and A. van Wijngaarden, Phys. Rev. Lett. **60**, 1002 (1988).

[3]M. S. Dewey and R. W. Dunford, Phys. Rev. Lett. **60**, 2014 (1988).

[4]P. J. Mohr, Phys. Rev. A **26**, 2338 (1982); in *Beam Foil Spectroscopy,* edited by I. A. Sellin and D. J. Pegg (Plenum, New York, 1976), p. 89.

[5]J. J. Bollinger and F. M. Pipkin, Rev. Sci. Instrum. **52**, 938 (1981).

[6]N. F. Ramsey, *Molecular Beams* (Oxford Univ. Press, London, 1956), p. 124.

[7]C. W. Fabjan and F. M. Pipkin, Phys. Rev. A **6**, 556 (1972).

[8]J. H. Shirley, Phys. Rev. **138**, B979 (1965).

[9]P. K. Majumder, Ph.D thesis, Harvard University, 1988 (unpublished).